Title
Structural patterns of the proximal femur in relation to age and hip fracture risk in women

Authors
Carballido-Gamio, Julio
Harnish, Roy
Saeed, Isra
et al.

Structural patterns of the proximal femur in relation to age and hip fracture risk in women

Julio Carballido-Gamio, Ph.D.[1], **Roy Harnish, M.S.**[1], **Isra Saeed, M.D.**[1], **Timothy Streeper, M.S.**[1], **Sigurdur Sigurdsson, Ph.D.**[2], **Shreyasee Amin, M.D.**[3,4], **Elizabeth J. Atkinson, M.S.**[5], **Terry M. Therneau, Ph.D.**[5], **Kristin Siggeirsdottir, M.S.**[2], **Xiaoguang Cheng, M.D.**[6], **L. Joseph Melton III, M.D.**[3,7], **Joyce Keyak, Ph.D.**[8], **Vilmundur Gudnason, M.D.**[2,9], **Sundeep Khosla, M.D.**[7], **Tamara B. Harris, M.D.**[10], and **Thomas F. Lang, Ph.D.**[1]

[1]Department of Radiology and Biomedical Imaging, University of California, San Francisco, San Francisco, CA, USA [2]Icelandic Heart Association, Kopavogur, Iceland [3]Division of Epidemiology, Department of Health Sciences Research, College of Medicine, Mayo Clinic, Rochester, MN, USA [4]Division of Rheumatology, Department of Internal Medicine, College of Medicine, Mayo Clinic, Rochester, MN, USA [5]Division of Biomedical Statistics and Informatics, Department of Health Sciences Research, College of Medicine, Mayo Clinic, Rochester, MN, USA [6]Department of Radiology, Beijing Ji Shui Tan Hospital, Beijing, China [7]Division of Endocrinology, Diabetes, Metabolism and Nutrition, Department of Internal Medicine, College of Medicine, Mayo Clinic, Rochester, MN, USA [8]Department of Radiological Sciences, University of California, Irvine, Irvine, CA, USA [9]University of Iceland, Reykjavik, Iceland [10]Intramural Research Program, National Institute on Aging, Bethesda, MD, USA

Abstract

Fractures of the proximal femur are the most devastating outcome of osteoporosis. It is generally understood that age-related changes in hip structure confer increased risk, but there have been few explicit comparisons of such changes in healthy subjects to those with hip fracture. In this study, we used quantitative computed tomography and tensor-based morphometry (TBM) to identify three-dimensional internal structural patterns of the proximal femur associated with age and with incident hip fracture. A population-based cohort of 349 women representing a broad age range (21–97 years) were included in this study, along with a cohort of 222 older women (mean age 79±7 years) with (n=74) and without (n=148) incident hip fracture. Images were spatially normalized to a standardized space, and age- and fracture-specific morphometric features were identified based on statistical maps of shape features described as local changes of bone volume. Morphometric features were visualized as maps of local contractions and expansions, and significance was displayed as Student's t-test statistical maps. Significant age-related changes included local expansions of regions low in volumetric bone mineral density (vBMD) and local contractions of regions high in vBMD. Some significant fracture-related features resembled an accentuated aging process, including local expansion of the superior aspect of the trabecular bone compartment in the femoral neck, with contraction of the adjoining cortical bone. However, other features were observed only in the comparison of hip fracture subjects with age-matched controls

Corresponding author: Thomas F. Lang, 185 Berry Street, Suite 350, San Francisco CA 94143, (415)-353-4552, Thomas.Lang@ucsf.edu.

including focal contractions of the cortical bone at the superior aspect of the femoral neck, the lateral cortical bone just inferior to the greater trochanter, and the anterior intertrochanteric region. Results of this study support the idea that the spatial distribution of morphometric features is relevant to age-related changes in bone and independently to fracture risk. In women, the identification by TBM of fracture-specific morphometric alterations of the proximal femur, in conjunction with vBMD and clinical risk factors, may improve hip fracture prediction.

Keywords

Osteoporosis; proximal femur; statistical parametric mapping; tensor-based morphometry (TBM); age; fracture

Introduction

Bone is a dynamic organ that exhibits structural adaptation to changes in its biochemical and biomechanical environment. Recent studies of the proximal femur using volumetric quantitative computed tomography (vQCT) and finite element modeling (FEM) have compared aspects of structure and strength in older and younger female subjects, showing that older women are characterized by larger bone size, lower trabecular volumetric bone mineral density (vBMD), thinner superior but not inferior femoral neck cortices, and lower whole bone strength [1–5]. Studies of proximal femur structure in women with hip fracture compared to age-matched controls have shown similar trends, with fractured women having larger cross-sectional areas, lower trabecular vBMD, thinner cortices in all subregions of the hip, and lower whole bone strength [6–8]. However, although age-related changes impart increased fragility to the proximal femur, the extent to which fracture-related variations in structure differ from age-related changes is still unclear.

In vQCT studies of the proximal femur, the ability to compare geometric features between individuals requires that analyses of geometric parameters, such as femoral neck cross sectional area, assume a general uniformity of outer bone shape, while cortical bone thickness measures assume similar cortical bone anatomy. However, the internal cancellous structure of the hip [9, 10] is often neglected or indirectly studied based on vBMD values of predefined volumes of interest. In this work, we quantify the three-dimensional (3D) internal structural patterns of the proximal femur in relation to age and incident hip fracture using vQCT images and a shape analysis technique known as tensor-based morphometry (TBM) [11]. For this purpose we studied two population-based cohorts: The first cohort included primarily Caucasian women across a broad range of age [1], while the second cohort included Caucasian women with and without incident hip fracture [12]. We will refer to these as the Aging Study and the Fracture Study, respectively. We used the same population-based cohorts in a recent study using voxel-based morphometry (VBM) and vQCT to study the spatial distribution of vBMD values in relation to age and incident hip fracture in women [13]. That study was based on the assumption of similar outer shapes of proximal femora between different subjects. The study presented here used TBM, which quantifies local differences in shape. Our goal was to examine, side-by-side, the internal structural patterns in the proximal femur that are associated with aging and with hip fracture to better understand normal aging and the pathophysiology of incident hip fracture.

Materials and Methods

Human Subjects

Aging Study—Using the medical records linkage system of the Rochester Epidemiology Project, 373 women were enrolled from an age-stratified random sample of Rochester, MN,

residents, and included in this study [1]. Mayo Clinic's Institutional Review Board, and the Committee on Human Research at the University of California, San Francisco, approved the study. Informed consent was obtained from all participants in the study, and the analyses were based on deidentified data. For analysis, women were divided into three subgroups based on their age: young (age<45 years), middle-age (45 age<60 years), and older (age 60 years).

Fracture Study—Using the AGES-Reykjavik Fracture Registry [14], a total of 222 women of the AGES Reykjavik cohort [12, 15] were included in this study. The AGES Reykjavik study is an ongoing population-based study of Icelandic women and men, where baseline CT scans of 5,500 subjects were obtained between 2002 and 2006, and subjects were followed for 4–7 years (mean 5 years). For this study, based on their fracture status, women were divided into two subgroups: controls (no hip fracture), and fracture (incident hip fracture but without documented hip fracture prior to CT imaging at baseline). The study was approved (VSN 00-063) by the National Bioethics Committee in Iceland and the Data Protection Authority, the Institutional Review Board of the Intramural Research Program of the National Institute on Aging, and the Committee on Human Research at the University of California, San Francisco. Informed consent was obtained from all participants in the study.

Imaging

Aging Study—Single-energy CT scans of both hip joints were obtained for each subject using a multi-detector CT scanner (Light Speed QX-I; GE Medical Systems, Wakesha, WI, USA) and a QCT calibration phantom (Mindways Inc., Austin, TX, USA) to convert Hounsfield Units (HU) to equivalent concentrations of K_2HPO_4. Images were reconstructed to in-plane voxel sizes of 0.74×0.74 mm^2, with slice thickness of 2.5 mm.

Fracture Study—CT scans of both hips were obtained for each subject at baseline using a 4-detector CT system (Sensation, Siemens Medical Systems, Erlangen, Germany) and a solid QCT calibration phantom (Image Analysis, Inc., Columbia, KY, USA) containing cells of 0, 75, and 150 mg/cm^3 equivalent concentration of calcium hydroxyapatite. Images were reconstructed to in-plane voxel sizes of 0.98×0.98 mm^2, with slice thickness of 1 mm.

Geometric and vBMD measures

Aging Study—Measures of vBMD and bone cross-sectional geometry were extracted from the femoral neck region as previously described in [1, 16]. From a single reformatted oblique section orthogonal to the femoral neck axis four parameters were evaluated in this study: Integral vBMD, Total Area, Cortical Area, Medullary Area and the ratio of the Cortical to the Total Area. These measures have been shown to be age- and sex-specific over life [1].

Fracture Study—Measures of vBMD and cortical structure that have been shown to predict hip fracture in cross-sectional [17] and prospective studies [18] were extracted from a volumetric region of the femoral neck as previously described in [19]. These included Integral vBMD, Total Volume, Cortical Volume, Medullary Volume and the ratio of the Cortical to Total Volumes.

Image Preprocessing

The left proximal femur was semi-automatically segmented from each CT scan on a slice-by-slice basis [7, 20], and images and their corresponding segmentations were upsampled to isotropic voxel sizes to match the in-plane voxel dimensions generating 3D representations of the proximal femur.

TBM

TBM is one of the most popular deformation-based approaches for analyzing macroscopic anatomy [11]. Briefly, in TBM, all images of the structure of interest in a given study are spatially normalized to a standardized space using image registration. First, an affine transformation is applied to translate, rotate, and scale (one scale for each dimension) the images. Then a nonlinear transformation is computed. The nonlinear step of the spatial normalization assigns a displacement vector to each voxel to accommodate anatomic variability. TBM processes these dense maps of displacement vectors, which are known as deformation fields, to generate feature maps representing shape in the form of local changes of volume. TBM then compares shape maps between two groups of subjects, or the same group of subjects at different time points, and detects subregions where shape is significantly associated with the effect of interest, making it possible to visualize group differences or longitudinal changes as statistical maps. Figure 1 shows a flow diagram summarizing the major steps of TBM.

In this study, spatial normalization was performed by concatenating multi-resolution affine (9-parameter) and multi-resolution nonlinear transformations [21]. Affine transformations were computed based on level-set representations of femoral surfaces using distance maps [22, 23], and nonlinear registrations were computed based on combined representations of distance maps for the background and gray-level values for the proximal femur (Figure 1) [24]. The standardized space consisted of a minimum deformation template (MDT) [25]. In this study, two MDTs were constructed, one to represent the average size, shape, and internal structure of the proximal femur of the young subgroup from the Aging Study (Young-MDT), and a second one to represent the average size, shape, and internal structure of the control subgroup from the Fracture Study (Control-MDT). Thus, spatially normalized images resembled the size, external shape, and internal structure of a MDT. Proximal femora of the young, middle-age, older, and control subgroups were spatially normalized to the Young-MDT, while proximal femora of the control and fracture subgroups were spatially normalized to the Control-MDT.

The dense deformation fields that nonlinearly accommodated the external and internal anatomic variability during spatial normalization were examined. For each voxel, spatial derivatives of the nonlinear deformations were calculated to construct a matrix known as the Jacobian matrix of the deformations. The determinant of the Jacobian matrix of the deformations is the metric that has been most studied in morphometric studies [26–28]. This expresses the resulting local volume change around each voxel in the image being deformed. If the determinant is equal to 1, it indicates no local change in volume; if the determinant is less than one, it indicates local contraction; and, if the determinant is larger than one, it indicates local expansion. The logarithm of the Jacobian determinant was quantitatively analyzed as the shape feature, since numerous studies have indicated its superior performance [29]. The implementation of nonlinear transformations was diffeomorphic [21], thus avoiding folding and, consequently, negative Jacobian determinants (disappearing volume).

Two different TBM analyses were performed: A whole-bone analysis, and a surface-based analysis. For the whole-bone analysis, the logs of the determinants of the Jacobian matrices were smoothed with an isotropic Gaussian kernel to ensure that each voxel contained the average shape from its local neighborhood and to compensate for the inexact nature of spatial normalization [30, 31]. For the surface-based analysis, the femoral surface was extracted from each deformed scan and represented as a triangulated mesh. The logs of the determinants of the Jacobian matrices representing local volumetric changes in a spherical neighborhood (radius=~2.75mm) around each vertex of the surface were averaged (for

reasons similar to those of the Gaussian smoothing in the whole-bone analysis) and placed onto the surface mesh for statistical analysis [28].

Statistical Analysis

Subject Characteristics—In the Aging Study, differences in height and weight between young, middle-age, and older women were evaluated using analysis of variance with Bonferroni correction for multiple-comparison correction. In the Fracture Study, differences in age, height, weight, and areal BMD (aBMD) by vQCT between control and fracture women were evaluated using analysis of variance. Differences were considered significant at $P<0.05$.

Geometric and vBMD measures—In the Aging Study, the association between age and vQCT measures of the femoral neck (Integral vBMD, Total Area, Cortical Area and Cortical/Total Area Ratio) was evaluated using general linear models with height and weight as covariates. In the Fracture Study, the relationship between fracture status and vQCT measures of the femoral neck (Integral vBMD, Total Volume, Cortical Volume and Cortical/Total Volume Ratio) was also evaluated using general linear models, however, age was also included as covariate in addition to height and weight. An association was considered significant at $P<0.05$.

TBM

Voxel-Wise Volume Differences—In the Aging Study, in order to visualize age-related internal structural differences, maps representing 3D mean percent volume differences of the middle-age and the older women with respect to the young women were generated. In the Fracture Study, a map representing 3D mean percent volume differences of the fracture women with respect to the control women was also generated to visualize fracture-related internal structural features. A fourth map was generated to depict mean percent volume differences of the control women from the Fracture Study with respect to the young women from the Aging Study. This map was computed to evaluate if women from the Fracture Study experienced similar age-related internal structural changes as older women from the Aging Study, and thus discern between age-related and fracture-related features.

Whole-Bone Statistical Analysis—Voxel-wise comparisons of shape features were performed between middle-age and young, and older and young women in the Young-MDT space, and between fracture and control women in the Control-MDT space. The fracture subgroup was compared to the control subgroup in the Control-MDT space because Studholme and colleagues demonstrated an improvement in spatial normalization when the reference atlas was age-matched [32]. Voxel-wise comparisons were done using a general linear model approach. The shape feature was used as the dependent variable, and group membership as the independent variable, yielding Student's t-test statistical maps (T-maps) that indicate regions significantly associated with age or with incident hip fracture. In the Aging Study, height and weight were included as covariates, while age, height, and weight were used in the Fracture Study [33–35]. False discovery rate (FDR) correction (q=0.05) was used to correct for multiple comparisons over the whole proximal femur [36].

Surface-Based Statistical Analysis—Similar subgroup comparisons to those of the whole-bone analysis were done for the surface shape maps by constraining the linear models to the vertices of the meshes, thus providing increased sensitivity [28].

Robustness—In order to test the robustness of the presented methodology, four additional MDTs were generated and four additional whole-bone statistical TBM analyses were performed. The additional MDTs were constructed based on the random subdivision of the

young and control subgroups into halves to generate two young MDTs (Young-MDT-1, n=47; Young-MDT-2, n=47) and two control MDTs (Control-MDT-1, n=74; Control-MDT-2, n=74). The four additional whole-bone statistical TBM comparisons were done between young and older women in the Young-MDT-1 and Young-MDT-2 spaces, and between older control and older fracture women in the Control-MDT-1 and Control-MDT-2 spaces.

Results

Subject Characteristics

In the Aging Study, 24 women were excluded due to problems with image quality, presence of pathologies in the proximal femur, or femoral segmentation problems, leaving a total of 349 women for this cohort. The young, middle-age, and older subgroups were composed then of 94, 98, and 157 women, respectively. The mean height was slightly smaller in women from the oldest age subgroups (means of 165, 164, and 160 cm, P<0.0001), and the mean weight was higher in women from the middle-age subgroup (72, 77, and 72 kg, P<0.05). In the Fracture Study, the control and fracture subgroups were composed of 148 and 74 women, respectively. The mean aBMD of women in the fracture subgroup was significantly lower than that of women in the control subgroup (P<0.0001). Table 1 summarizes the descriptive statistics for the different subgroups of the Aging and Fracture Studies.

Geometric and vBMD measures

Results of linear models comparing vQCT femoral neck vBMD and geometry measures between younger and older women in the Aging Study, and between control women and women with incident hip fracture in the the Fracture Study, are summarized in Table 2. In the Aging Study, older women had lower integral femoral neck vBMD, Cortical Area and Cortical/Total Area ratios and larger Total and Medullary femoral neck areas (all differences p<0.01). In the fracture study, women with incident hip fracture had lower femoral neck integral vBMD (p<0.001), Cortical Volume (p<0.05) and Cortical/Total Volume ratio (p<0.001), but higher Medullary Volume (p<0.05) and a non-significant trend towards higher Total Volume.

TBM

MDTs—Figure 2 shows coronal cross-sections of the Young-MDT where voxel intensities have been color-coded (gray tones=low intensity; red tones=medium intensity; yellow tones=high intensity) to highlight the internal structures of the proximal femur studied in this work. The clear patterns observed in Figure 2A and annotated in Figure 2B are the result of stable an accurate registrations based on combined representations of voxel-intensities for the proximal femur and distance maps for the background.

Voxel-Wise Volume Differences—Age-related internal structural changes of the proximal femur are shown in Figure 3 as maps of voxel-wise mean percent volume differences of women from the middle-age (Figure 3A), older (Figure 3B), and control (Figure 3C) subgroups with respect to women from the young subgroup. The 3D views and the coronal cross-section of the older subgroup map (Figure 3B) show further accentuation of the spatial features seen in the map of the middle-age subgroup (Figure 3A), while the views of the map of the control subgroup from the Fracture Study (Figure 3C) show similar spatial features and dynamic ranges as the older map from the Aging Study (Figure 3B). In Figure 3, the main age-related patterns depict (A) expansions of 1) the superolateral region of the femoral head (e_1), 2) the inferolateral region of the femoral head (e_2), 3) the trabecular bone compartment in the greater trochanter (e_3), 4) the central aspect of the trabecular bone

compartment in the neck (e_4), and 5) the trabecular bone compartment in the proximal shaft (e_5); and (B) contractions of 1) the region above the epiphyseal scar (c_1), 2) the compressive trabecular bands (c_2), 3) the cortical bone at the superior aspect of the femoral neck (c_3), 4) the inferior aspect of the trabecular bone compartment of the neck (c_4), and 5) the secondary arcuate system (Arc2 [10]) forming the lateral part of the intertrochanteric arch (c_5). Smaller changes were seen as contractions of the inferior cortical bone of the femoral neck (sc_1), and of the lateral cortical bone just inferior to the greater trochanter (sc_2).

Figure 4 shows the fracture-related internal structural features of the proximal femur as maps of voxel-wise mean percent volume differences of women from the fracture subgroup with respect to women from the control subgroup. In this figure, women from the fracture subgroup showed patterns similar to those observed in women from the older subgroup, such as expansions of the superolateral and inferolateral regions of the femoral head, the central region of the femoral neck, and the trochanteric and proximal shaft trabecular bone compartments. Likewise, contractions were seen in the region above the epiphyseal scar, the compressive trabecular bands, the Arc2, and the cortical bone at the inferior aspect of the femoral neck. However, some of the fracture-related features were distinct from the age-related patterns observed in Figure 3: 1) focal contraction of the anterior aspect of the intertrochanteric region (fc_1), 2) focal contraction of the cortical bone at the superior aspect of the femoral neck (fc_2), 3) focal contraction of the lateral cortical bone just inferior to the greater trochanter (fc_3), and 4) focal expansion of the superior aspect of the trabecular bone compartment of the femoral neck (fe_1).

It is important to note that the voxel-wise mean percent volume differences depicted in Figures 3 and 4 are not indicative of differences in bone size. The differences are local, because they were calculated based on the deformation fields that were computed after the 9-parameter affine transformation of the spatial normalization process, which uses scaling to remove overall differences in bone size.

Whole-Bone Statistical Analysis—Different 3D views and coronal cross-sections of the T-maps of the morphometric comparisons in the Aging Study between middle-age and young women, and between older and young women, are shown in Figures 5A and 5B, respectively. These Tmaps were adjusted for inter-group differences in height and weight, and voxels were assigned transparency based on their T-values, from full transparency for non-significant voxels, to full opacity for minimum and maximum T-values. Most of the age-related morphometric changes depicted in Figure 3 were significant in Figures 5A and 5B, and significant regions in the older subgroup (Figure 5B) were consistent to those observed in the middle-age subgroup (Figure 5A), but with approximately a twofold increase in T-values.

The T-map of the Fracture Study shown in Figures 5C and 5D was computed based on the comparison between fracture and control women (adjusted for age, height, and weight), and voxel transparency was also applied as in Figures 5A and 5B. Local shape was significantly associated with incident hip fracture in multiple regions that overlapped those associated with aging. These morphometric features and locations were seen as further (A) expansions of 1) the superolateral and inferolateral regions of the femoral head, and 2) the medullary compartment in the proximal shaft; and as further (B) contractions of 1) the region above the epiphyseal scar, and 2) the inferior cortex. However, the focal contractions (fc_1, fc_2, fc_3) and expansion (fe_1) observed in Figure 4, which were distinct from the morphometric features observed with aging, also showed significance.

Figure 6 illustrates, side-to-side, the location in the proximal femur of significant age-related and fracture-related morphometric changes, and also distinguishes between the cortical and

trabecular bone compartments. Figures 6A and 6B show 3D internal views of the anterior halves of the T-maps that were obtained from the voxel-wise morphometric comparisons of older and young women, and fracture and control women, respectively, blended with their corresponding MDTs.

Surface-Based Statistical Analysis—T-maps of the morphometric comparisons of the surfacebased analysis are shown in Figure 7. Comparisons between middle-age and young women, and between older and young women from the Aging Study are shown in Figures 7A and 7B, respectively, while the vertex-wise comparisons between control and fracture women from the Fracture Study are shown in Figures 7C and 7D. In Figure 7, non-significant vertices were displayed in gray.

Similar to the whole-bone analysis shown in Figure 5, regions indicating contractions and expansions significantly associated with aging in the older subgroup (Figure 7B), were consistent to those observed in the middle-age subgroup (Figure 7A). Likewise, some regions indicating contractions and expansions significantly associated with incident hip fracture (Figures 7C–7D) overlapped regions that were significantly associated with aging; however, the focal cortical bone contractions observed in the whole-bone analysis were also significant in the surface-based analysis.

Robustness—Coronal cross-sections of the T-maps of the three comparisons between young and older women, and of the three comparisons between control and fracture women are shown in Figure 8. T-maps indicating the local association between shape and age show similar patterns and dynamic ranges in the three young spaces (Young-MDT-1 in Figure 8A; Young MDT-2 in Figure 8B; and Young-MDT in Figure 8C). Similarly, common features and dynamic ranges can be observed in the T-maps indicating the local association between shape and hip fracture in the three controls spaces (Control-MDT-1 in Figure 8D; Control-MDT-2 in Figure 8E; and Control-MDT in Figure 8F).

Discussion

In this study, we identified morphometric differences between young and older women that were shared between fractured and non-fractured subjects, as well as some features that were unique to fracture subjects. These differences were distinguished with an approach that differed from previous studies in its use of a statistical atlas-based technique, TBM. Based on voxel-by-voxel analysis of the image data, this technique permits identification of the regions of significant internal expansion and contraction that are associated with age group and fracture status. The novelty of this study also involved the inclusion of young, middle-age, normal older, and fracture older women, the focus on the internal rather than on the outer structure of the proximal femur, and the use of an image-data driven approach to extract both trabecular and cortical macroscopic features from this data set. This study differs from our previous work on VBM [13] because the nature of the analyzed features was different: While VBM quantifies spatial differences of vBMD values, TBM quantifies spatial differences of shape.

The age-related morphometric changes that we have documented are in agreement with several other published reports that examined both cadaveric bones as well as other population cohorts [3, 8–10, 37]. Figure 3 provides insight into the evolution of several distinct age-related morphometric features of the proximal femur, as illustrated by the yellow-green and purple-blue regions, respectively corresponding to expansions and contractions of tissue on a per voxel basis (Figures 5A–5B and 7A–7B). Consistent with previous studies using vQCT [2], thinning of the superior cortical margin as a function of age was observed. Since this thinning was well established in middle-age women, and did

not show pronounced changes between the middle-age and older women, it is possible that this thinning process is already complete by middle age. The superior femoral neck cortex receives primary impact from lateral falls, and our results would be consistent with a recent cross-sectional study carried out in the same subjects, which used finite element modeling (FEM) and simulated sideways fall loading to show that a large part of the age-related decline in whole bone strength had already occurred by completion of the menopause [37]. It is also possible that this process continues into old age but that the changes to this extremely thin structure are too small to be detected by vQCT. Other features appeared to show a gradual evolution from middle to old age. These included contraction of regions high in vBMD, e.g. the principal compressive band of trabeculae and what appear to be portions of the anterior and posterior cortex, and expansion of regions low in vBMD, e.g. the central aspect of the femoral neck (Ward's triangle), the trochanteric medullary bone, and at the border of the articular surface. Because the TBM analysis is carried out after scaling is used to remove overall differences in bone size, the medullary expansions and cortical contractions would be consistent with an overall process of cortical thinning.

Two patterns of morphometric differences between subjects with incident hip fracture and age-matched controls were observed. The first pattern comprised a set of features resembling an advanced aging process. These included fracture-related expansions of medullary regions and contractions of cortical regions and of high-vBMD trabecular compartments. The other set of features comprised focal contractions of cortical bone (Figures 4, 5D and 7D) and a focal expansion of the superior aspect of the trabecular bone compartment in the femoral neck (Figures 4 and 5D). Focal morphometric changes associated with incident hip fracture observed in this study were consistent with previous studies. For example, regarding the focal contraction of cortical bone in the superior aspect of the femoral neck (fc_2 in Figure 4; also seen in Figures 5D and 7D), Mayhew and colleagues suggested that cortical thinning in the upper femoral neck increases hip fragility, and they hypothesized that lower loads in this zone on common daily activities such as walking could be a potential explanation for this effect [2]. Later, in a study of incident hip fracture, Johannesdottir and colleagues detected cortical bone thinning in the same region based on a 2D cross-section of the neck using vQCT scans [38]. In a recent cross-sectional study using statistical parametric mapping (SPM) by Poole et al., focal cortical thinning was also observed in the superior aspect of the femoral neck in women with femoral neck fracture [8]. In the same study, focal thinning in the lateral cortical bone just inferior to the greater trochanter was observed in subjects with femoral neck fracture, also in agreement with the focal contraction seen in the same region in this study (fc_3 in Figure 4; also seen in Figures 5D and 7D). Although it was not significant, Poole et al. detected cortical thinning in the anterior aspect of the intertrochanteric region, which was in agreement with a local contraction observed in our study in the same area (fc_1 in Figure 4; also seen in Figures 5D and 7D). Unfortunately, no previous SPM analysis has been applied to study the trabecular bone compartment in the proximal femur, so the focal expansion observed in the superior aspect of the trabecular bone compartment of the femoral neck could not be compared with other studies. However, this focal expansion could potentially be explained by the hypothesis of Mayhew and colleagues [2]. The extent to which the morphologic patterns observed in this study affect bone strength is a question requiring evaluation techniques such as FEM. However, the superior aspect of the femoral neck and the trochanteric area are regions commonly associated with hip fracture.

We have validated the robustness of the whole technique presented in this study: generation of MDTs, spatial normalization of QCT scans, and statistical analysis, by adding 4 additional comparisons to the study. Results indicate that our pipeline is robust, since very similar patterns were identified between the different T-maps in the Aging and Fracture Studies (Figure 8) despite the fact that they were generated with different MDTs and new

sets of image registrations. This robustness was the result of nonlinear registrations that had the following characteristics: 1) diffeomorphic; 2) based on femoral segmentations; 3) based on a combination of distance fields for the background and gray-level values for the proximal femur; facilitating the convergence of the algorithm, its accuracy, and its stability. Furthermore, TBM yielded similar trends to those observed using conventional vQCT geometric parameters, i.e. contraction of the cortices and expansion of the local trabecular volumes in older and fracture women compared to younger and control women, respectively, with the advantage of providing localized statistical information of these morphometric changes, and thus enabling their visualization as feature maps.

TBM and similar techniques can be employed to describe age- and fracture–related variations in structure, but it should be noted that they could also be used in fracture prediction models. Although global characteristics such as integral bone density, size and geometry, or regional features such as compartmental BMD or trabecular bone architecture represent the current sources of image characteristics used in prediction models, statistical-atlas based techniques provide a new source of potential features. Voxel-based morphometry (VBM) was used by Li and colleagues to identify subregions in the proximal femur where vBMD was significantly associated with hip fracture [6]. SPM was used by Poole and colleagues to identify subregions in the proximal femur where cortical bone thickness was significantly associated with femoral neck or trochanteric fracture [8]. Regions significantly associated with hip fracture can then be used for fracture discrimination [6], or principal component analysis (PCA) can be applied to a statistical atlas of features to develop prediction models of fracture [39–41] or bone quality [24]. Simpler approaches based on image similarity have also been explored [42], as well as PCA in hip radiographs to predict incident hip fracture based on 2D features of bone shape [43]. In this study, TBM and vQCT are proposed as potential tools to extract relevant internal morphometric features for hip fracture prediction, which are not provided by any of the approaches mentioned above.

This study had both strengths and limitations. Its major strengths were the use of two populationbased cohorts, the prospective design of the Fracture Study, and the integration of internal structural features into statistical atlases of two of the most relevant aspects in the study of osteoporosis: aging and hip fracture. An important limitation was that hip fracture types were not differentiated, thus preventing the investigation of internal structural differences between subcapital, neck, and trochanteric fractures. The second limitation was that the analysis included primarily Caucasian women, so our findings may not be applicable to men and other ethnicities. Another limitation of our study was that the femoral neck vQCT vBMD and structural parameters were analyzed with different methods in the Aging and Fracture Studies, with the former analyzing a single femoral neck cross-section and the latter a volume of tissue. However, these methods of computation have shown consistent results in cross-sectional studies of aging. Similar to a previous vQCT analysis of the Aging Study cohort [1], the volume-derived vQCT methods in the fracture study has shown age-related decreases in vBMD and cortical to total volume ratios, and increases of total and medullary volumes [3, 12].

In conclusion, in this work we have used vQCT and TBM to investigate side-to-side two of the most relevant aspects in the study of osteoporosis in women, aging and incident hip fracture, in an anatomical site of utmost importance, the proximal femur. Regions where local shape was significantly associated with age or with incident hip fracture were identified and visualized as local contractions or expansions. Our results indicate that although certain internal structural features of the proximal femur associated with risk of hip fracture in women resemble an advanced aging process, other features are unique and focal. Furthermore, our results support the idea that the spatial distribution of morphometric features is relevant to fracture risk. When employed in conjunction with feature extraction

techniques such as PCA, we believe that TBM and associated approaches, in combination with vBMD and clinical risk factors, may better predict the incidence of hip fracture.

Acknowledgments

References

1. Riggs BL, Melton Iii LJ 3rd, Robb RA, Camp JJ, Atkinson EJ, Peterson JM, et al. Population-based study of age and sex differences in bone volumetric density, size, geometry, and structure at different skeletal sites. J Bone Miner Res. 2004; 19:1945–1954. [PubMed: 15537436]

2. Mayhew PM, Thomas CD, Clement JG, Loveridge N, Beck TJ, Bonfield W, et al. Relation between age, femoral neck cortical stability, and hip fracture risk. Lancet. 2005; 366:129–135. [PubMed: 16005335]

3. Meta M, Lu Y, Keyak JH, Lang T. Young-elderly differences in bone density, geometry and strength indices depend on proximal femur sub-region: a cross sectional study in Caucasian-American women. Bone. 2006; 39:152–158. [PubMed: 16459156]

4. Ito M, Wakao N, Hida T, Matsui Y, Abe Y, Aoyagi K, et al. Analysis of hip geometry by clinical CT for the assessment of hip fracture risk in elderly Japanese women. Bone. 2010; 46:453–457. [PubMed: 19735752]

5. Poole KE, Mayhew PM, Rose CM, Brown JK, Bearcroft PJ, Loveridge N, et al. Changing structure of the femoral neck across the adult female lifespan. J Bone Miner Res. 2010; 25:482–491. [PubMed: 19594320]

6. Li W, Kornak J, Harris T, Keyak J, Li C, Lu Y, et al. Identify fracture-critical regions inside the proximal femur using statistical parametric mapping. Bone. 2009; 44:596–602. [PubMed: 19130910]

7. Keyak JH, Sigurdsson S, Karlsdottir G, Oskarsdottir D, Sigmarsdottir A, Zhao S, et al. Male-female differences in the association between incident hip fracture and proximal femoral strength: a finite element analysis study. Bone. 2011; 48:1239–1245. [PubMed: 21419886]

8. Poole KE, Treece GM, Mayhew PM, Vaculik J, Dungl P, Horak M, et al. Cortical thickness mapping to identify focal osteoporosis in patients with hip fracture. PLoS One. 2012; 7:e38466. [PubMed: 22701648]

9. Kerr R, Resnick D, Sartoris DJ, Kursunoglu S, Pineda C, Haghighi P, et al. Computerized tomography of proximal femoral trabecular patterns. J Orthop Res. 1986; 4:45–56. [PubMed: 3950808]

10. Elke RP, Cheal EJ, Simmons C, Poss R. Three-dimensional anatomy of the cancellous structures within the proximal femur from computed tomography data. J Orthop Res. 1995; 13:513–523. [PubMed: 7674067]

11. Davatzikos C, Vaillant M, Resnick SM, Prince JL, Letovsky S, Bryan RN. A computerized approach for morphological analysis of the corpus callosum. J Comput Assist Tomogr. 1996; 20:88–97. [PubMed: 8576488]

12. Sigurdsson G, Aspelund T, Chang M, Jonsdottir B, Sigurdsson S, Eiriksdottir G, et al. Increasing sex difference in bone strength in old age: The Age, Gene/Environment Susceptibility-Reykjavik study (AGES-REYKJAVIK). Bone. 2006; 39:644–651. [PubMed: 16790372]

13. Carballido-Gamio J, Harnish R, Saeed I, Streeper T, Siggurdsson S, Amin S, et al. Proximal femoral density distribution and structure in relation to age and hip fracture risk in women. J Bone Miner Res. 2012 Accepted.

14. Siggeirsdottir K, Aspelund T, Sigurdsson G, Mogensen B, Chang M, Jonsdottir B, et al. Inaccuracy in self-report of fractures may underestimate association with health outcomes when compared

with medical record based fracture registry. Eur J Epidemiol. 2007; 22:631–639. [PubMed: 17653601]

15. Harris TB, Launer LJ, Eiriksdottir G, Kjartansson O, Jonsson PV, Sigurdsson G, et al. Age, Gene/ Environment Susceptibility-Reykjavik Study: multidisciplinary applied phenomics. Am J Epidemiol. 2007; 165:1076–1087. [PubMed: 17351290]

16. Camp, JJ.; Karwoski, RA.; Stacy, MC.; Atkinson, EJ.; Khosla, S.; Melton Iii, LJ., 3rd, et al., editors. A system for the analysis of whole-bone strength from helical CT images. SPIE Medical Imaging; 2004.

17. Cheng X, Li J, Lu Y, Keyak J, Lang T. Proximal femoral density and geometry measurements by quantitative computed tomography: association with hip fracture. Bone. 2007; 40:169–174. [PubMed: 16876496]

18. Black DM, Bouxsein ML, Marshall LM, Cummings SR, Lang TF, Cauley JA, et al. Proximal femoral structure and the prediction of hip fracture in men: a large prospective study using QCT. J Bone Miner Res. 2008; 23:1326–1333. [PubMed: 18348697]

19. Lang T, LeBlanc A, Evans H, Lu Y, Genant H, Yu A. Cortical and trabecular bone mineral loss from the spine and hip in long-duration spaceflight. J Bone Miner Res. 2004; 19:1006–1012. [PubMed: 15125798]

20. Keyak JH, Rossi SA, Jones KA, Skinner HB. Prediction of femoral fracture load using automated finite element modeling. J Biomech. 1998; 31:125–133. [PubMed: 9593205]

21. Vercauteren T, Pennec X, Perchant A, Ayache N. Non-parametric diffeomorphic image registration with the demons algorithm. Med Image Comput Comput Assist Interv. 2007; 10:319–326. [PubMed: 18044584]

22. Reinertsen I, Descoteaux M, Drouin S, Siddiqi K, Collins DL. Vessel driven correction of brain shift. Lect Notes Comput Sc. 2004; 3217:208–216.

23. Suh JW, Wyatt CL. Deformable registration of prone and supine colons for CT colonography. Conf Proc IEEE Eng Med Biol Soc. 2006; 1:1997–2000. [PubMed: 17946082]

24. Fritscher K, Grunerbl A, Hanni M, Suhm N, Hengg C, Schubert R. Trabecular bone analysis in CT and X-ray images of the proximal femur for the assessment of local bone quality. IEEE Trans Med Imaging. 2009; 28:1560–1575. [PubMed: 19520636]

25. Hua X, Leow AD, Levitt JG, Caplan R, Thompson PM, Toga AW. Detecting brain growth patterns in normal children using tensor-based morphometry. Hum Brain Mapp. 2009; 30:209–219. [PubMed: 18064588]

26. Hua X, Leow AD, Parikshak N, Lee S, Chiang MC, Toga AW, et al. Tensor-based morphometry as a neuroimaging biomarker for Alzheimer's disease: an MRI study of 676 AD, MCI, and normal subjects. Neuroimage. 2008; 43:458–469. [PubMed: 18691658]

27. Brun CC, Lepore N, Pennec X, Lee AD, Barysheva M, Madsen SK, et al. Mapping the regional influence of genetics on brain structure variability--a tensor-based morphometry study. Neuroimage. 2009; 48:37–49. [PubMed: 19446645]

28. Rajagopalan V, Scott J, Habas PA, Kim K, Corbett-Detig J, Rousseau F, et al. Local tissue growth patterns underlying normal fetal human brain gyrification quantified in utero. J Neurosci. 2011; 31:2878–2887. [PubMed: 21414909]

29. Lepore N, Brun C, Chou YY, Chiang MC, Dutton RA, Hayashi KM, et al. Generalized tensor-based morphometry of HIV/AIDS using multivariate statistics on deformation tensors. IEEE Trans Med Imaging. 2008; 27:129–141. [PubMed: 18270068]

30. Ashburner J, Friston KJ. Voxel-based morphometry--the methods. Neuroimage. 2000; 11:805–821. [PubMed: 10860804]

31. Mechelli A, Price CJ, Friston KJ, Ashburner J. Voxel-based morphometry of the human brain: Methods and applications. Curr Med Imaging Rev. 2005; 1:105–113.

32. Studholme, C.; Cardenas, V.; Weiner, M., editors. Multi scale image and multi scale deformation of brain anatomy for building average brain atlases. SPIE Medical Imaging; 2001.

33. Chung MK, Dalton KM, Alexander AL, Davidson RJ. Less white matter concentration in autism: 2D voxel-based morphometry. Neuroimage. 2004; 23:242–251. [PubMed: 15325371]

34. Campbell LE, Daly E, Toal F, Stevens A, Azuma R, Catani M, et al. Brain and behaviour in children with 22q11.2 deletion syndrome: a volumetric and voxel-based morphometry MRI study. Brain. 2006; 129:1218–1228. [PubMed: 16569671]

35. Barnes J, Ridgway GR, Bartlett J, Henley SM, Lehmann M, Hobbs N, et al. Head size, age and gender adjustment in MRI studies: a necessary nuisance? Neuroimage. 2010; 53:1244–1255. [PubMed: 20600995]

36. Genovese CR, Lazar NA, Nichols T. Thresholding of statistical maps in functional neuroimaging using the false discovery rate. Neuroimage. 2002; 15:870–878. [PubMed: 11906227]

37. Lang TF, Sigurdsson S, Karlsdottir G, Oskarsdottir D, Sigmarsdottir A, Chengshi J, et al. Age-related loss of proximal femoral strength in elderly men and women: The Age Gene/Environment Susceptibility Study - Reykjavik. Bone. 2012; 50:743–748. [PubMed: 22178403]

38. Johannesdottir F, Poole KE, Reeve J, Siggeirsdottir K, Aspelund T, Mogensen B, et al. Distribution of cortical bone in the femoral neck and hip fracture: a prospective case-control analysis of 143 incident hip fractures; the AGES-REYKJAVIK Study. Bone. 2011; 48:1268–1276. [PubMed: 21473947]

39. Li, W.; Kornak, J.; Harris, T.; Lu, Y.; Cheng, X.; Lang, T., editors. Hip fracture risk estimation based on principal component analysis of QCT atlas: a preliminary study. SPIE Medical Imaging; 2009.

40. Schuler B, Fritscher KD, Kuhn V, Eckstein F, Link TM, Schubert R. Assessment of the individual fracture risk of the proximal femur by using statistical appearance models. Med Phys. 2010; 37:2560–2571. [PubMed: 20632568]

41. Whitmarsh T, Fritscher KD, Humbert L, Del Rio Barquero LM, Roth T, Kammerlander C, et al. A statistical model of shape and bone mineral density distribution of the proximal femur for fracture risk assessment. Med Image Comput Comput Assist Interv. 2011; 14:393–400. [PubMed: 21995053]

42. Li W, Kornak J, Harris TB, Keyak J, Li C, Lu Y, et al. Bone fracture risk estimation based on image similarity. Bone. 2009; 45:560–567. [PubMed: 19414074]

43. Baker-LePain JC, Luker KR, Lynch JA, Parimi N, Nevitt MC, Lane NE. Active shape modeling of the hip in the prediction of incident hip fracture. J Bone Miner Res. 2011; 26:468–474. [PubMed: 20878772]

Highlights

We studied age- and hip fracture-related alterations of proximal femoral structure.

We used quantitative computed tomography imaging and tensor-based morphometry (TBM).

We studied healthy women (aged 21–97 years) and elderly women with hip fracture.

Fracture women showed age-related and also uniquely fracture-related structural changes.

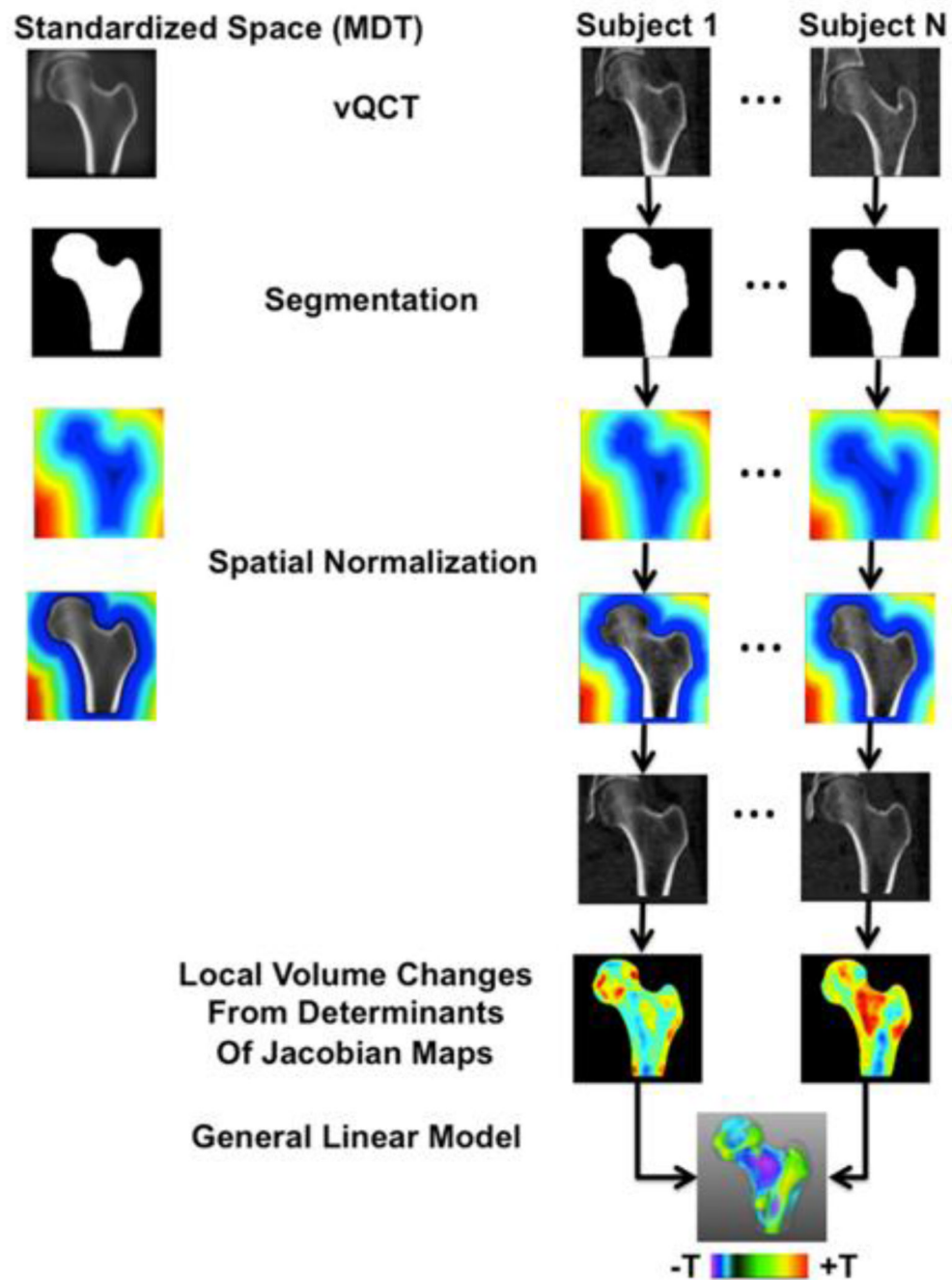TBM may provide structure biomarkers to identify women at high risk for hip fracture.

Figure 1.
Flow diagram illustrating the different steps of the TBM technique used in this study. The left proximal femur was segmented from all scans. Images representing the femoral shape as distance maps, and combined images where the proximal femur was represented with gray-level values and the background with distance maps, were generated and used for spatial normalization. All scans of a given subgroup were spatially normalized to a standardized space represented as a MDT. The amount of deformation that was needed in each voxel to match the standardized space was computed and represented as maps of contractions-expansions, which were used to compare local shape differences on a voxel-by-voxel basis between subgroups. Comparisons were made using a general linear model approach

generating T-maps, which indicated regions where local shape was significantly associated with age or with incident hip fracture.
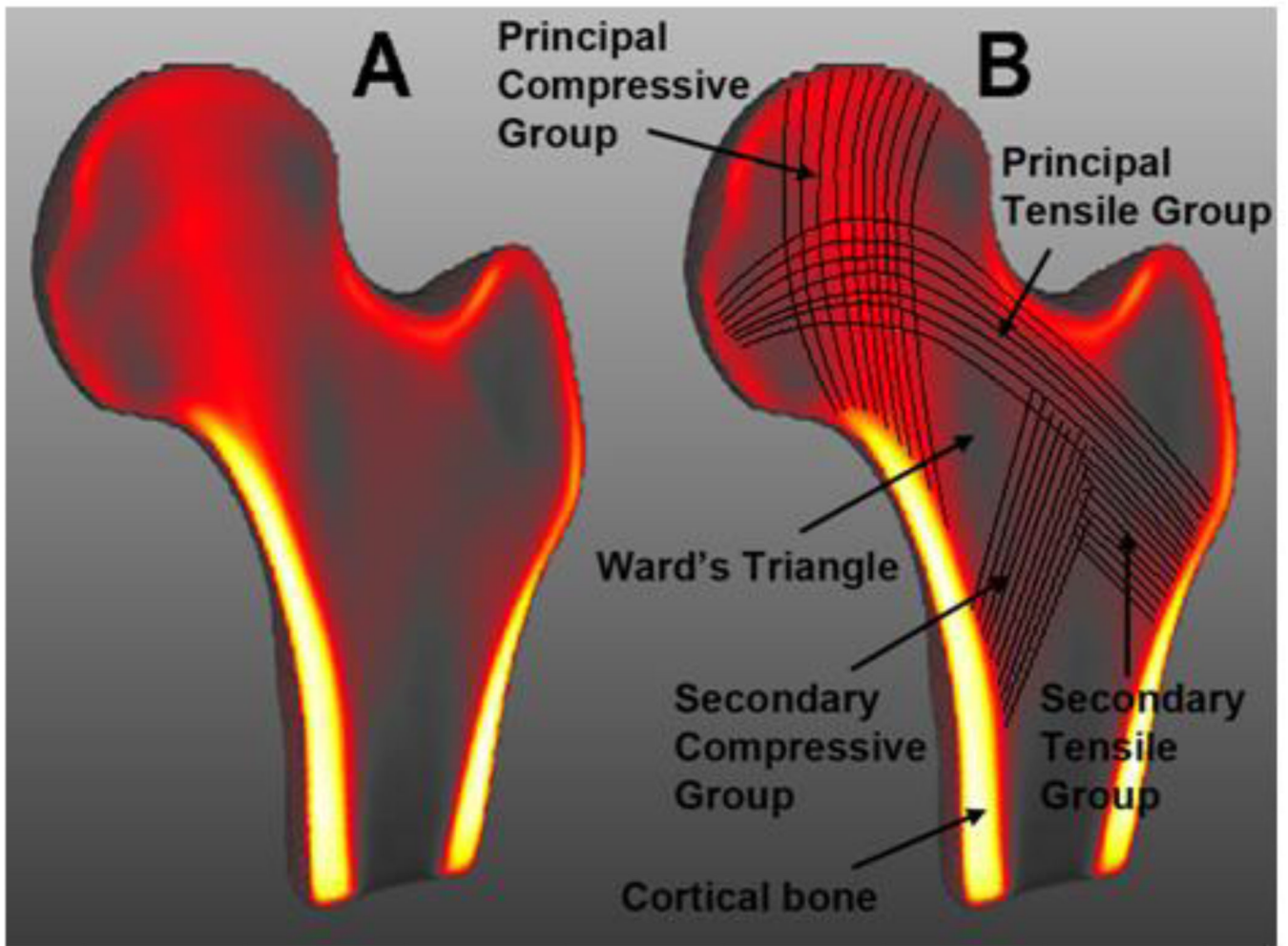
Figure 2.
(A) Coronal cross-section of the minimum deformation template representing the average size, shape, and internal structure of young women. (B) Coronal cross-section of A indicating the major internal structural features of the proximal femur studied in this work. Voxels are color-coded based on their intensities; from low intensity values represented with gray tones, through medium intensity values with red tones, to high intensity values with yellow tones.
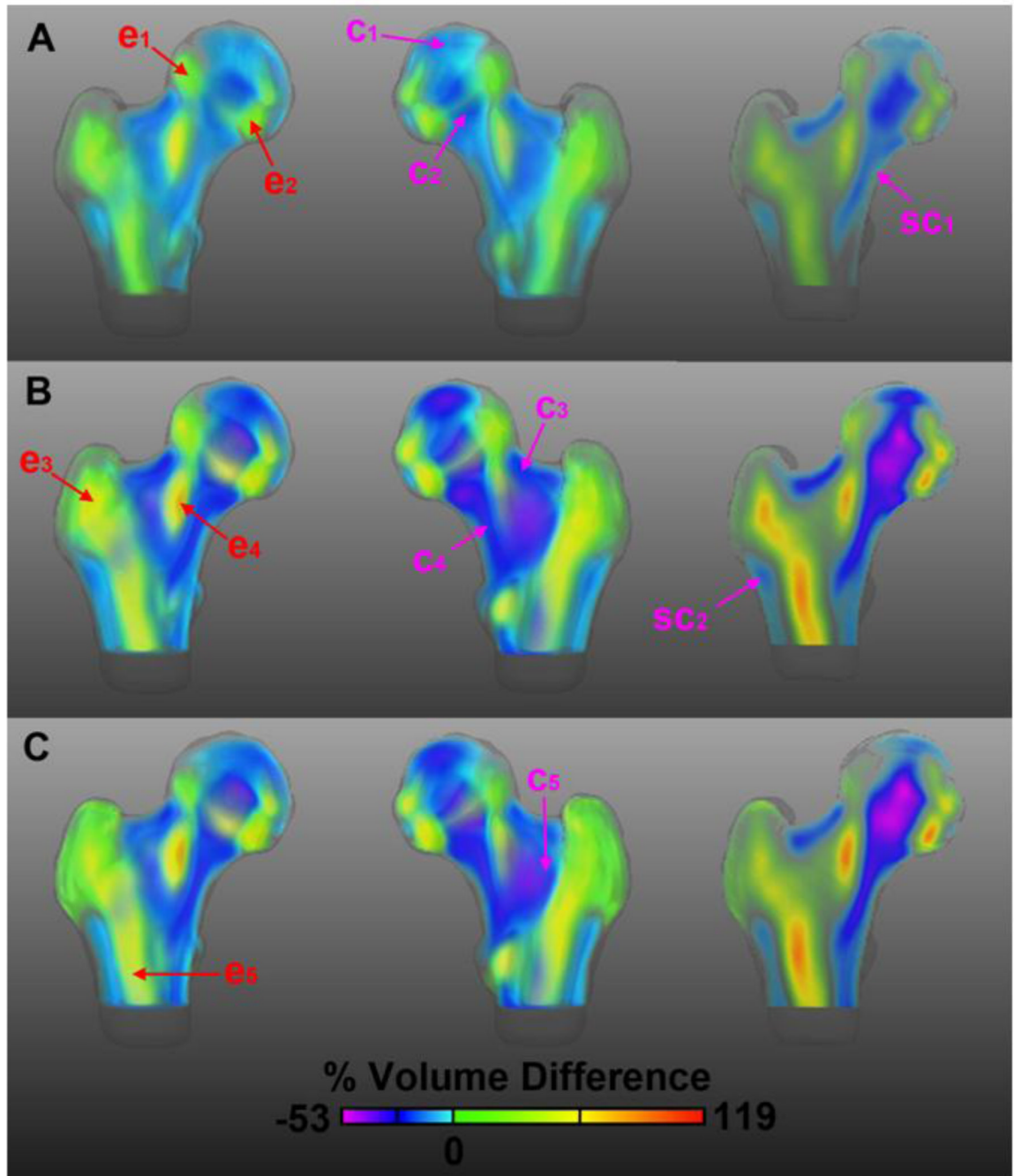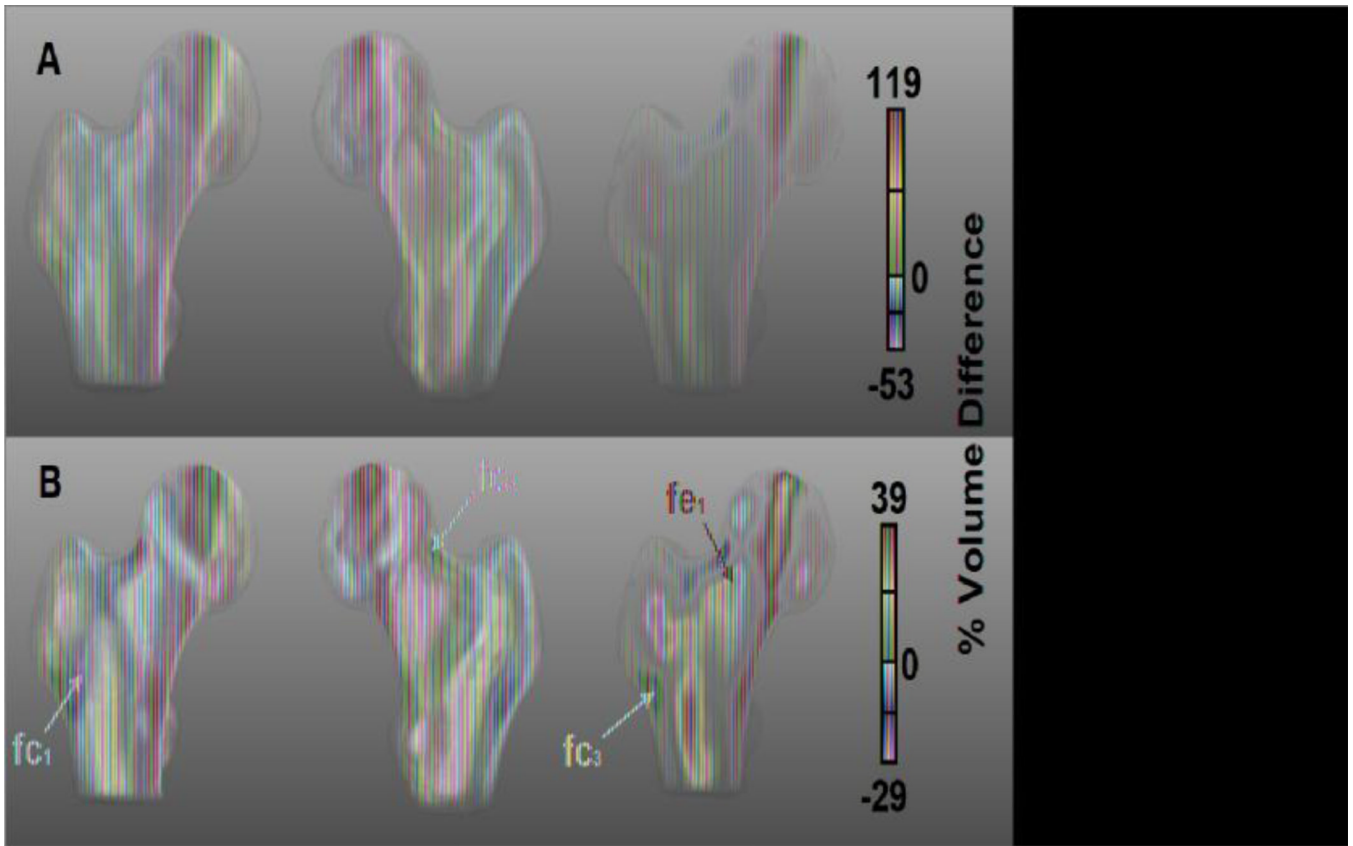
Figure 3.
Anterior, posterior, and coronal cross-sectional views of age-related morphometric changes in the proximal femur. The maps depict mean local volume differences of the middle-age subgroup from the Aging Study (A), the older subgroup from the Aging Study (B), and the control subgroup from the Fracture Study (C), with respect to the young subgroup from the Aging Study. Red and magenta arrows point to the main patterns of local volume expansion and contraction, respectively. The color scale is based on the dynamic range of the comparison in B. Differences were calculated prior to the application of the logarithm.

Figure 4.
Anterior, posterior, and coronal cross-sectional views of fracture-related morphometric features in the proximal femur. The maps depict mean local volume differences of the fracture subgroup with respect to the control subgroup, both from the Fracture Study. Magenta and red arrows point to regions where the fracture subgroup showed local volume contractions and expansions, respectively. Maps in A use the color scale of Figure 3, which corresponds to the dynamic range of the comparison between older and young women from the Aging Study. Maps in B use the color scale corresponding to the dynamic range of the comparison between control and fracture women from the Fracture Study. Differences were calculated prior to the application of the logarithm.
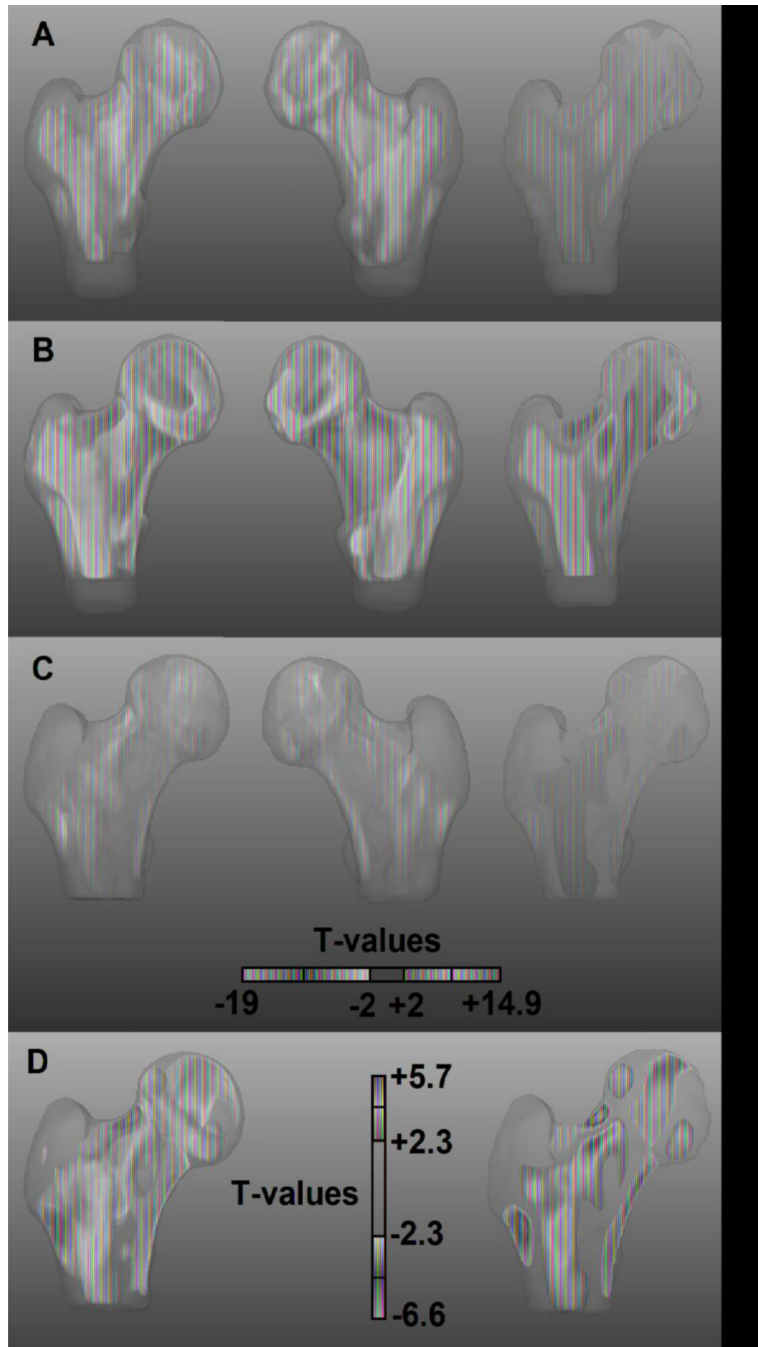
Figure 5.
Anterior, posterior, and coronal cross-sectional views of T-maps showing regions of the proximal femur where local shape was significantly associated with age (A and B; Aging Study) or incident hip fracture (C and D; Fracture Study). Consistency was found between the Tmaps in A and B, which were computed based on the comparisons of the middle-age and older subgroups, respectively, with the young subgroup. The views of the T-maps shown in C and D, which was computed based on the comparison between fracture and control women, show focal regions significantly associated with incident hip fracture. The color scale in A, B and C was based on the dynamic range of the comparison in B. The color

scale in D was based on the dynamic range of the comparison in C-D. Transparency was applied to each voxel based on its T-value.
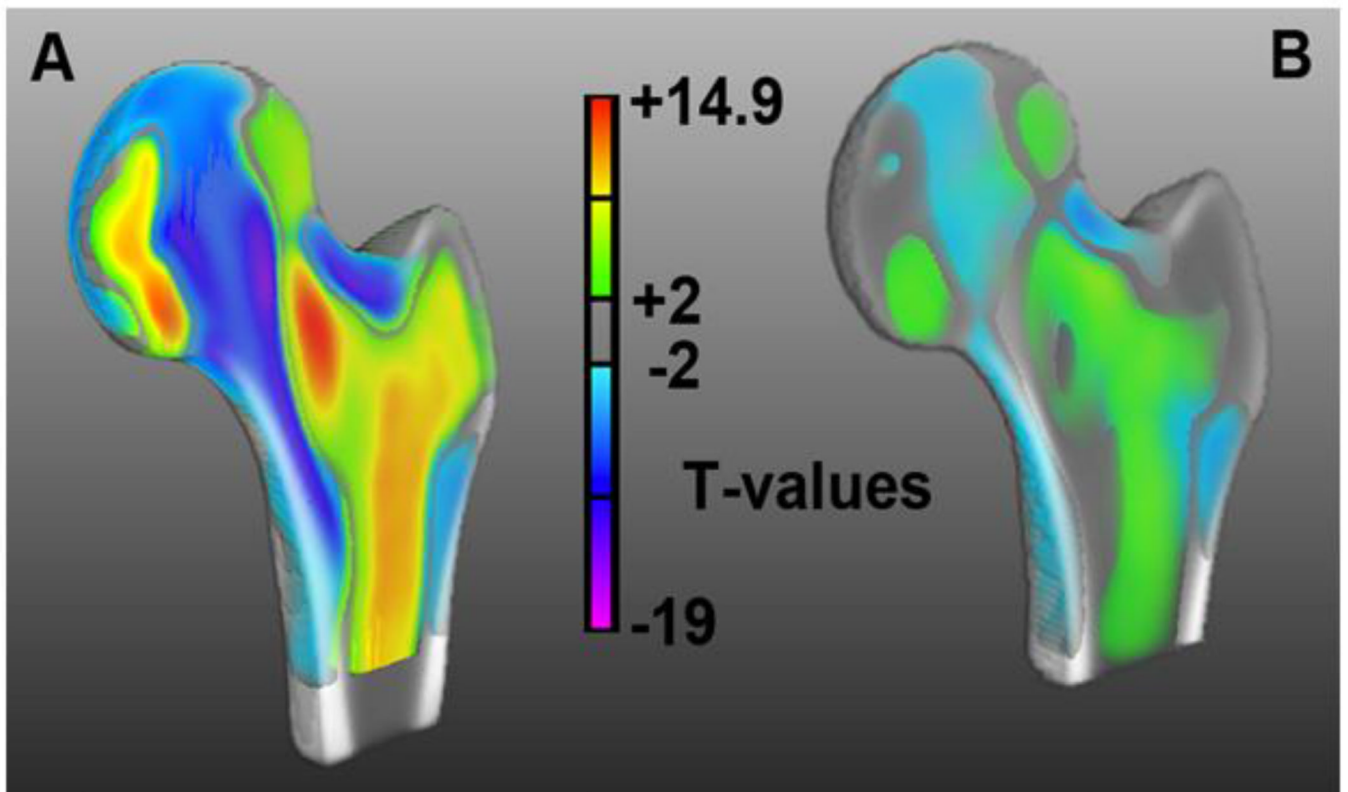
Figure 6.
Side-to-side visualization of regions where local shape was significantly associated with age or with incident hip fracture. (A) Internal view of the anterior half of the proximal femur where the Young-MDT and the T-map of the comparison between older and young women were blended. (B) Internal view of the anterior half of the proximal femur where the Control-MDT and the T-map of the comparison between fracture and control women were blended. The color scale is based on the dynamic range of the comparison in A. Transparency was applied to each voxel based on its T-value.
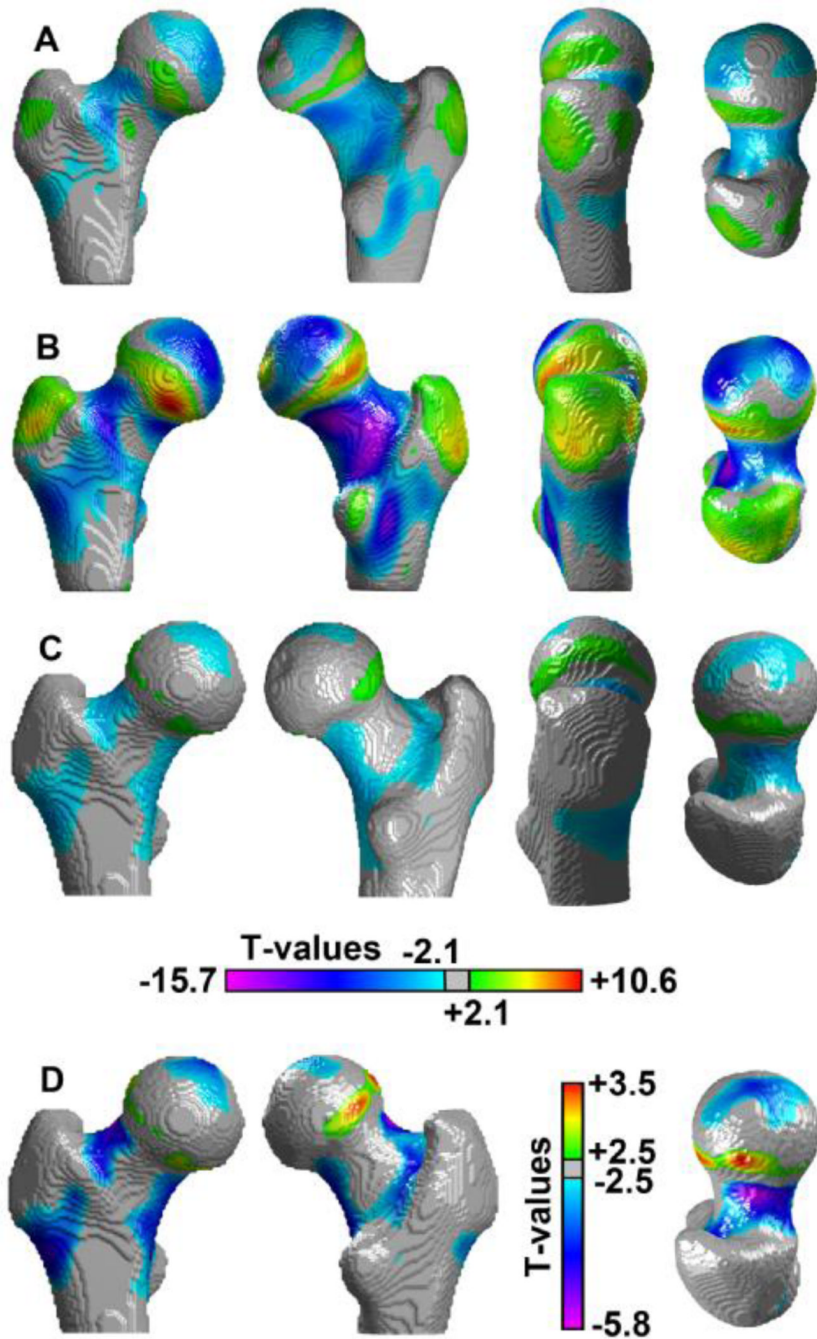
Figure 7.
Anterior, posterior, lateral, and superior views of T-maps showing regions of the proximal femoral surface where local shape was significantly associated with age (A and B; Aging Study) or with incident hip fracture (C and D; Fracture Study). Consistency was found between the T-maps in A and B, which were computed based on the comparisons of the middleage and older subgroups, respectively, with the young subgroup. The views of the T-map shown in C and D, which was computed based on the comparison between fracture and control women, show focal regions significantly associated with incident hip fracture. The color scale in A, B and C was based on the dynamic range of the comparison in B. The color

scale in D was based on the dynamic range of the comparison in C-D. Non-significant vertices were displayed in grey.
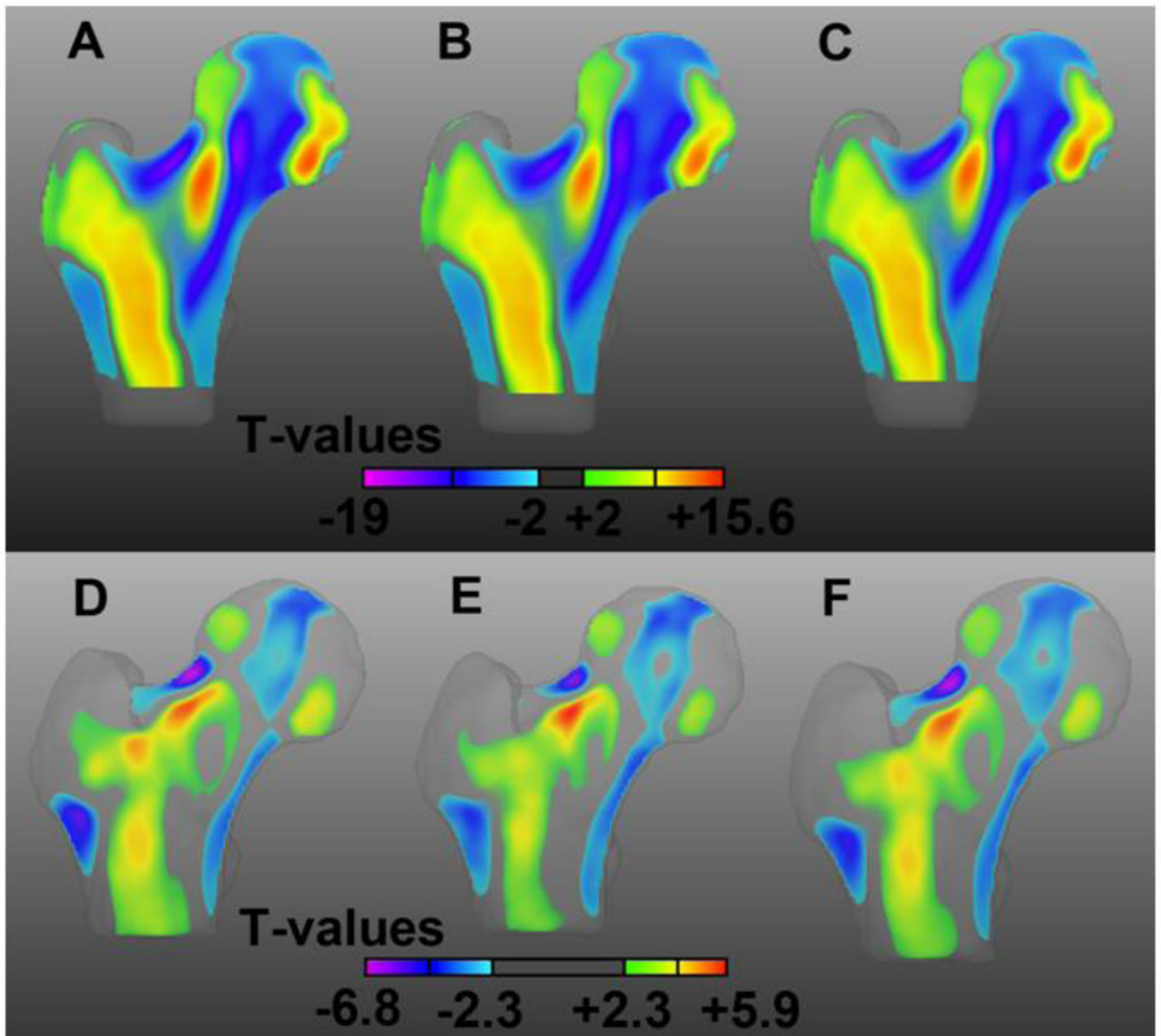
Figure 8.
Coronal cross-sections of the T-maps of the comparisons between young and older women in the Young-MDT-1 space (A), in the Young-MDT-2 space, and in the Young-MDT space; and of the comparisons between control and fracture women in the Control-MDT-1 space (D), in the Control-MDT-2 space (E), and in the Control-MDT space. Transparency was applied to each voxel based on its T-value.

Table 1

Descriptive Statistics for Women of the Aging and Fracture Studies.

Subgroup	Measure	N[a]	Range	Mean	SD	P
Young	Age	94	21 – 44	34	7	
	Height	94	151 – 178.1	165.4	6.0	0.0001[b]
	Weight	94	44.9 – 113.5	72.1	17.0	
Middle-Age	Age	98	45 – 59	52	4	
	Height	98	153.7 – 179.7	163.9	5.8	0.0001[b]
	Weight	98	50.6 – 151.2	77.3	18.4	0.05[c]
Older	Age	157	60 – 97	73	9	
	Height	157	143 – 179.5	160.3	6.4	0.0001[b]
	Weight	157	40.5 – 119.9	71.8	13.7	0.05[c]
Controls	Age	148	67 – 92	79	6	
	Height	147	139.2 – 172.9	159.2	5.6	
	Weight	147	37.2 – 112	68.4	13.7	
	aBMD	148	0.337 – 1.239	0.694	0.155	0.0001
Fracture	Age	74	67 – 93	79	6	
	Height	73	145.1 – 173.4	159.6	6.1	
	Weight	73	39.2 – 111.2	64.5	15.1	
	aBMD	74	0.392 – 0.960	0.604	0.123	0.0001

Units: Age (years), height (cm), weight (kg), and aBMD (g/cm^2).

SD = Standard deviation.

[a] Differences in the number of data points for each measure within each subgroup are due to missing data.

[b] Significantly different from the older subgroup in the Aging Study.

[c] Significantly different between the middle-age and older subgroups in the Aging Study.

Table 2

Femoral neck integral vBMD and geometric measures[#] of the Aging and Fracture Studies. Results given as means ± standard deviation.

Subgroup	Int.vBMD (mg/cm³)	Total Area (cm²)	Cortical Area (cm²)	Medullary Area (cm²)	Cortical/Total Area
Young	404.51466.209	6.4530.890	2.2770.265	4.1750.823	0.3580.052
Older	294.04362.029 ***	6.9411.044 ***	2.1180.329 **	4.8230.945 ***	0.3090.049 ***

	Int.vBMD (mg/cm³)	Total Vol (cm³)	Cortical Vol (cm³)	Medullary Vol (cm³)	Cortical/Total Vol
Controls	240.74755.213	14.7912.578	5.6431.249	9.1482.087	0.3840.069
Fracture	207.14836.473 ***	15.2753.141	5.2241.055 *	10.0522.397 *	0.3450.042 ***

[#] vBMD and structural parameters in Aging study were computed in a single cross-section of the femoral neck and for the Fracture Study were computed in a volumetric region of interest. Comparisons were done in the form of general linear models adjusted by height and weight for the Aging Study, and height, weight, and age for the Fracture Study.

*
p<0.05

**
p<0.01

***
p<0.001